ACS OMEGA

Article

Cite This: ACS Omega 2018, 3, 15692−15701

http://pubs.acs.org/journal/acsodf

Bimacrocyclic Effect in Anion Recognition by a Copper(II) Bicyclam Complex

Michele Invernici,[†] Carlo Ciarrocchi,[†] Daniele Dondi,[†] Luigi Fabbrizzi,*[,†] Simone Lazzaroni,[†] Maurizio Licchelli,*[,†] Massimo Boiocchi,[‡] and Marco Bonizzoni*[,§]

[†]Dipartimento di Chimica, Università di Pavia, via Taramelli 12, I-27100 Pavia, Italy

[‡]Centro Grandi Strumenti, Università di Pavia, via Bassi 21, I-27100 Pavia, Italy

[§]Department of Chemistry, The University of Alabama, Tuscaloosa 35487, Alabama, United States

Supporting Information

ABSTRACT: The dicopper(II) complex of the bimacrocyclic ligand *α*,*α*′-bis(5,7-dimethyl-1,4,8,11-tetraazacyclotetradecan-6-yl)-*o*-xylene, **2**, interacts with selected anions in dimethyl sulfoxide solution according to two different modes: (i) halides (Cl^-, Br^-, and I^-) and N_3^- coordinate the two metal centers at the same time between the two macrocyclic subunits that face each other and (ii) anionic species that do not fit the bridging coordination mode (e.g., NCO^-, SCN^-, CH_3COO^-, NO_3^-, and $H_2PO_4^-$) interact with copper(II) ions only at the "external" positions or their interaction is too weak to be detected. Occurrence of the bridging interaction is demonstrated by X-ray crystallographic studies performed on the adduct formed by $[Cu_2(\mathbf{2})]^{4+}$ with azide and by electron paramagnetic resonance investigation, as the anion coordination between the two copper(II) centers induces spin−spin coupling. Isothermal titration calorimetry experiments performed on $[Cu_2(\mathbf{2})]^{4+}$ and, for comparison, on [(5,7-dimethyl-6-benzyl-1,4,8,11-tetraazacyclotetradecane)copper(II)], representing the mononuclear analogue, allowed determination of thermodynamic parameters (log *K*, Δ*H*, and *T*Δ*S*) associated with the considered complex/anion equilibria. Thermodynamic data showed that adducts formed by $[Cu_2(\mathbf{2})]^{4+}$ with halides and azide benefit from an extra stability that can be explained on the basis of the anion advantage of simultaneously binding the two metal centers, i.e., in terms of the bimacrocyclic effect.

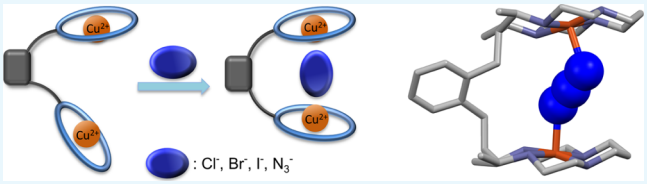

INTRODUCTION

Anion recognition is a well-established research topic, still attracting much interest in the field of supramolecular chemistry.[1] Starting from the pioneering studies carried out on cage-shaped receptors by Park & Simmons[1a] and Lehn,[1b] a very large number of artificial receptors and chemosensors for anionic species have been designed and investigated.[2] The recognition process can be based on a variety of host−guest interactions, including coordinative ones.[3] Metal−ligand interactions have been used in efficient anion receptors that include complexes with coordinatively unsaturated metal centers; this often results in very strong binding of guest anions at these open positions. Moreover, the better-defined directional character of metal−ligand bonds (particularly if compared to electrostatic interactions) may impose geometrical constraints that contribute to increasing recognition selectivity.[4] Several examples of metal complexes applied in the recognition of anionic species have also been described as "cascade" receptors.[3a−c] Metal complexes of polyamines, either linear or branched (e.g., tren), can be conveniently used as binding subunits in the design of anion receptors and chemosensors,[5] although they are usually labile and can undergo demetalation in the presence of excess anions or under acidic conditions (due to the protonation of the amine groups). On the contrary, cyclic amines and particularly cyclam-like ligands form inert complexes (e.g., with Cu^{II} and Ni^{II}) that do not undergo demetalation even under severe conditions, such as in strongly acidic solutions (e.g., a lifetime of 30 years has been evaluated for $[Ni(cyclam)]^{2+}$ in 1 M aqueous $HClO_4$).[6]

The coordination chemistry of dinuclear complexes, particularly of systems containing two transition metal ions separated by a relatively short distance (3.5−7.0 Å), has also attracted much interest during the last decades because of their involvement in a variety of biochemical and industrial processes.[7] The presence of two metal ions at a suitable distance can favor the coordination of small molecules, anions, and/or organic substrates and grant catalytic activity for certain reactions, for example, reduction of CO_2[8] and O_2.[9]

In particular, octaamine **2** represents an interesting example of bimacrocyclic ligand, consisting of two dimethyl-cyclam subunits in a trans-III conformation, bridged by an ortho-xylyl group. Both methyl groups on each cyclam ring are in the equatorial position with respect to the chair conformation of the six-membered chelate rings, causing an axial orientation of the xylylene group and consequently favoring the face-to-face

Received: July 19, 2018
Accepted: October 31, 2018
Published: November 16, 2018

DOI: 10.1021/acsomega.8b01710
ACS Omega 2018, 3, 15692−15701

arrangement of the two macrocyclic subunits.[10] The corresponding dinuclear complexes are able to combine the high inertness toward demetalation of the cyclam-like analogues with the capability of the pincer-like structure to chelate anions between the two metal centers.[10,11]

The dinickel(II) complex of ligand **2** was studied in the solid state by Endicott and co-workers,[11] who demonstrated that it shows an extreme versatility in the magnetic behavior, depending on the nature of the anion bound between the two facing metallocyclam subunits. Recently, we have studied the interaction of $[Ni_2(\mathbf{2})]^{4+}$ with halides and pseudohalides (azide, cyanate, and thiocyanate) in dimethyl sulfoxide (DMSO).[12] Figure 1 shows the possible positions where the

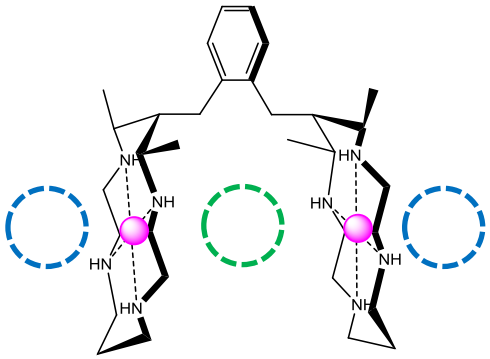

Figure 1. Schematic representation of the face-to-face structural arrangement adopted by dinuclear complexes of **2**. Anions could be coordinated simultaneously by two metal centers (inner position, green dashed circle) and/or by one metal ion (outer positions, blue dashed circles), the latter being equivalent to binding to a mononuclear complex.

anions can be coordinated by the dinuclear complex. Our spectrophotometric and voltammetric studies disclosed two main behavior modes: (i) pseudohalides preferentially interact outside the intermetallic cavity of the bimacrocyclic complex, benefiting from coordination to the metal ion of the dinuclear complex to the same extent as the analogous mononuclear species, $[Ni(\mathbf{1})]^{2+}$ and (ii) halides benefit from coordination to a greater extent when they bind the dinuclear complex because they are included in the intermetallic cavity and interact with two metal centers at the same time. We previously defined the "bimacrocyclic effect"[12] as the extra-stability displayed by complex/anion adducts in which anionic guests occupy the space between the two macrocyclic subunits, when compared to the adduct with the related mononuclear complex.

Recently, we have also investigated the interaction of the dicopper complex of ligand **2**, $[Cu_2(\mathbf{2})]^{4+}$, with selected anions in water, observing a substantial lack of selectivity in the recognition process. In particular, the examination of enthalpy and entropy terms, which were unbalanced or contrasting, disclosed that the contributions due to hydration/dehydration processes overcame any favorable effect because of the nature of the receptor (e.g., steric complementarity).[13]

Given the relevance of this result for a correct comprehension of the anion recognition process, we decided to investigate the interaction between $[Cu_2(\mathbf{2})]^{4+}$ and different anions in nonaqueous media, in order to confirm (or not) the major role of solvation/desolvation processes in solvents other than water. The study, performed in comparison with the mononuclear analogue, $[Cu(\mathbf{1})]^{2+}$, was restricted to DMSO solutions because of the poor solubility of the dinuclear complex in less polar solvents (e.g., MeCN, alcohols). In addition, we aimed to confirm the existence of a possible bimacrocyclic effect even in the complex/anion adducts formed by $[Cu_2(\mathbf{2})]^{4+}$ as previously observed for the analogous dinickel species.

Hence, we report the results obtained by using a range of experimental techniques according to the receptor-substrate approach. In particular, isothermal titration calorimetry (ITC) experiments and UV−vis spectrophotometric titrations provided information about stability of complex/anion adducts and related thermodynamic parameters (log K, ΔH, and $T\Delta S$), while electron paramagnetic resonance (EPR) measurements indicated the bridged or nonbridged nature of adducts. In fact, owing to copper(II) one-electron paramagnetism, complex $[Cu_2(\mathbf{2})]^{4+}$ could favor spin−spin coupling between its two copper centers in the presence of coordinated bridging anions, allowing to shed light on the mechanism of the anion−dinuclear complex interaction. Ligand-mediated spin−spin coupling processes have been previously investigated in different dinuclear complexes.[14] Moreover, a direct insight on the solid-state structural features of receptor/anion adducts is provided by X-ray crystallographic studies performed on the complex formed by $[Cu_2(\mathbf{2})]^{4+}$ with azide.

Table 1. EPR Parameters for $[Cu(\mathbf{1})](ClO_4)_2$ and $[Cu_2(\mathbf{2})](ClO_4)_4$ Determined in the Presence of Excess Anions (7 Equiv) in a Frozen Solution (DMSO, 120 K)

anion	complex	No. peaks[a]	spin−spin coupling	g_{II}	A_{II} [10^{-4} cm^{-1}]	D_{II} [10^{-4} cm^{-1}]
Cl^-	$[Cu(\mathbf{1})]^{2+}$	4	no	2.15	195	
	$[Cu_2(\mathbf{2})]^{4+}$	10[c]	yes	2.14	93	155
Br^-	$[Cu(\mathbf{1})]^{2+}$	4	no	2.15	195	
	$[Cu_2(\mathbf{2})]^{4+}$	10[c]	yes	2.11	96	140
I^-	$[Cu(\mathbf{1})]^{2+}$	4	no	2.15	195	
	$[Cu_2(\mathbf{2})]^{4+}$	10[c]	yes	2.20	96	92
N_3^-	$[Cu(\mathbf{1})]^{2+}$	4	no	2.15	195	
	$[Cu_2(\mathbf{2})]^{4+}$	10[c]	yes	2.14	94	147.5
NCO^-	$[Cu(\mathbf{1})]^{2+}$	4	no	2.15	190	
	$[Cu_2(\mathbf{2})]^{4+}$	4[b]	no	2.13	212	
CH_3COO^-	$[Cu(\mathbf{1})]^{2+}$	4	no	2.15	195	
	$[Cu_2(\mathbf{2})]^{4+}$	4[b]	no	2.12	205	

[a]Number of expected peaks = $2NI + 1$ (N, number of equivalent nuclei felt by the electron; I, nuclear spin quantum number). [b]Two groups of four overlapped lines. [c]Two groups of seven lines where four of them are overlapped.

DOI: 10.1021/acsomega.8b01710
ACS Omega 2018, 3, 15692−15701

RESULTS AND DISCUSSION

EPR Studies. EPR spectra were measured on frozen DMSO (120 K) solutions of $[Cu(\mathbf{1})](ClO_4)_2$ and $[Cu_2(\mathbf{2})](ClO_4)_4$ in the presence of increasing amounts (0, 0.5, 1, 2, and 7 equiv) of different anions (chloride, bromide, iodide, azide, cyanate, and acetate) that were added as the corresponding tetrabutylammonium (TBA^+) salts. Collected data are summarized in Table 1.

The spectrum of $[Cu(\mathbf{1})]^{2+}$ shows the typical four-line pattern in the parallel region (Figure 2a) expected for coupling

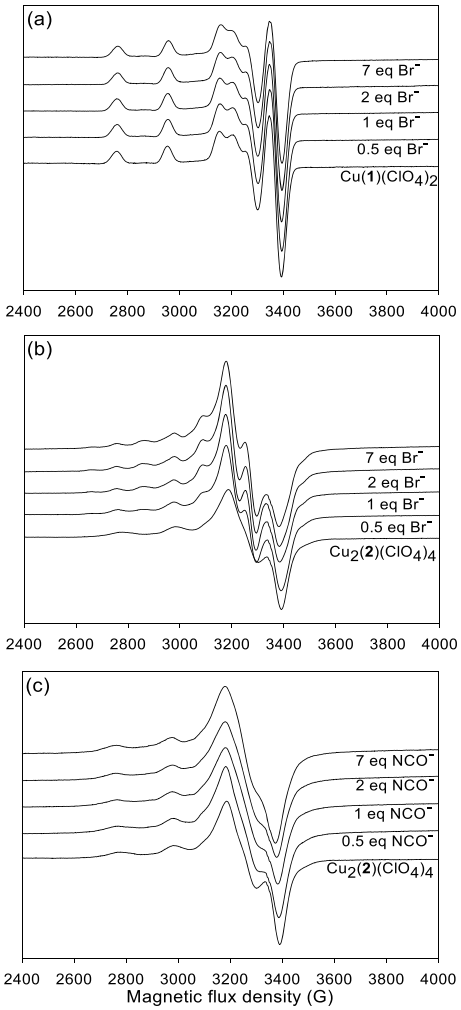

Figure 2. Experimental EPR spectra of a solution of (a) $[Cu(\mathbf{1})](ClO_4)_2$ (5×10^{-4} M) with increasing amounts of Br^-, (b) a solution of $[Cu_2(\mathbf{2})](ClO_4)_4$ (5×10^{-4} M) with increasing amounts of Br^-, and (c) with increasing amounts of NCO^-.

of one electron with the 3/2 spin of a copper(II) nucleus ($2NI + 1 = 4$, where N is the number of equivalent nuclei felt by the electron and I is the nuclear spin quantum number). The spectrum of $[Cu_2(\mathbf{2})]^{4+}$ also displays a four-line pattern (Figure 2b,c) because the two Cu^{2+} nuclei are not in communication with each other, thus each unpaired electron feels only one copper center, developing two overlapped groups of four lines.

The mononuclear complex still displays the four-line pattern when increasing amounts (0.5, 1, 2, 7 equiv) of any investigated anions are added. Spectra recorded on the solution of $[Cu(\mathbf{1})](ClO_4)_2$ with different amounts of bromide are shown in Figure 2a, whereas spectra obtained in the presence of other anions are reported in Figure S1 (Supporting Information). The EPR spectrum of the dinuclear complex is only slightly affected by the presence of cyanate and acetate (see Figures 2c and S2), whereas chloride, bromide, iodide, and azide make the spectrum assume the typical aspect of a triplet state, in which the metal−metal interaction is much greater than the hyperfine interaction, and the value of A_{II} is about half of that of the mononuclear complex, indicating a delocalization of the unpaired electrons ($S = 1/2$) over two equivalent copper centers. Spectra recorded on a frozen DMSO solution of $[Cu_2(\mathbf{2})]^{4+}$ with different amounts of bromide are shown in Figure 2b, whereas spectra concerning other anions are reported in Figure S2. The spectra of $[Cu_2(\mathbf{2})]^{4+}$ measured in the presence of anions that mediate the metal−metal interaction consist of two septuplets ($2NI + 1 = 2 \times 2 \times 3/2 + 1 = 7$), but just 10 lines can be identified instead of the expected 14 because 5 of them fall very close to each other and are indistinguishable (Figure 2b). The barycenter of the two septuplets is separated by a value of $2D_{II}$.

It should be noted that the addition of 0.5 equiv of chloride, bromide, or iodide, is enough to induce a change in the spectrum of the dicopper(II) complex, indicating that the first anion is coordinated between the two metal centers, bringing them closer and acting as a bridge, thus inducing spin−spin coupling. In the case of azide, the spin−spin coupling can be first noticed after the addition of 2 equiv of anion and may be due to a weaker interaction (see the next section for the stability constants of the bimacrocyclic complex/anion adducts). In the presence of large excess of halides and azide (7 equiv), the 10 lines are still visible in the EPR spectra, which indicate that the anion still remains inside the cavity and enables the spin−spin coupling. Cyanate and acetate do not induce any metal−metal interaction (see spectra in Figures 2c and S2, respectively), suggesting that they are coordinated only at the external positions of the bimacrocyclic complex.

Calorimetric Studies. Studies of the anion-binding properties of complex species $[Cu(\mathbf{1})]^{2+}$ and $[Cu_2(\mathbf{2})]^{4+}$ in pure DMSO were performed by ITC. In a typical experiment, a solution of the envisaged complex in DMSO was titrated by a solution of the investigated anion dissolved in the same solvent as (TBA)X salt ($X = Cl^-$, Br^-, I^-, N_3^-, NCO^-, CH_3COO^-, SCN^-, and NO_3^-). No heat effect was observed during the ITC titrations performed on both mono- and dinuclear complexes with NCS^- and NO_3^-, suggesting that the interaction with these anionic species is too weak to be detected. Figure 3 reports the thermograms and the ITC profiles (obtained by AFFINImeter software)[15] corresponding to the ITC titration of $[Cu(\mathbf{1})](ClO_4)_2$ with Cl^-, Br^-, N_3^-, and NCO^- (data for titration with I^- and CH_3COO^- are shown in Figure S3).

$[Cu(\mathbf{1})]^{2+}$ can coordinate the first equivalent of anion (1:1 adduct) according to a square-pyramidal geometry, binding the anion in the axial position. Sequentially, the mononuclear complex can coordinate the second equivalent of anion (1:2 complex) exploiting an elongated octahedral geometry, with both anions in an axial position, one anion for each side (Figure S4). In the cases of Cl^-, Br^-, NCO^-, and CH_3COO^-, we obtained the best fitting by assuming the occurrence of two stepwise equilibria, corresponding to the formation of 1:1 (eq 1) and 1:2 (eq 2) complex/anion adducts.

$$[Cu(1)]^{2+} + X^- \rightleftharpoons [Cu(1)X]^+ \quad (1)$$

DOI: 10.1021/acsomega.8b01710
ACS Omega 2018, 3, 15692−15701

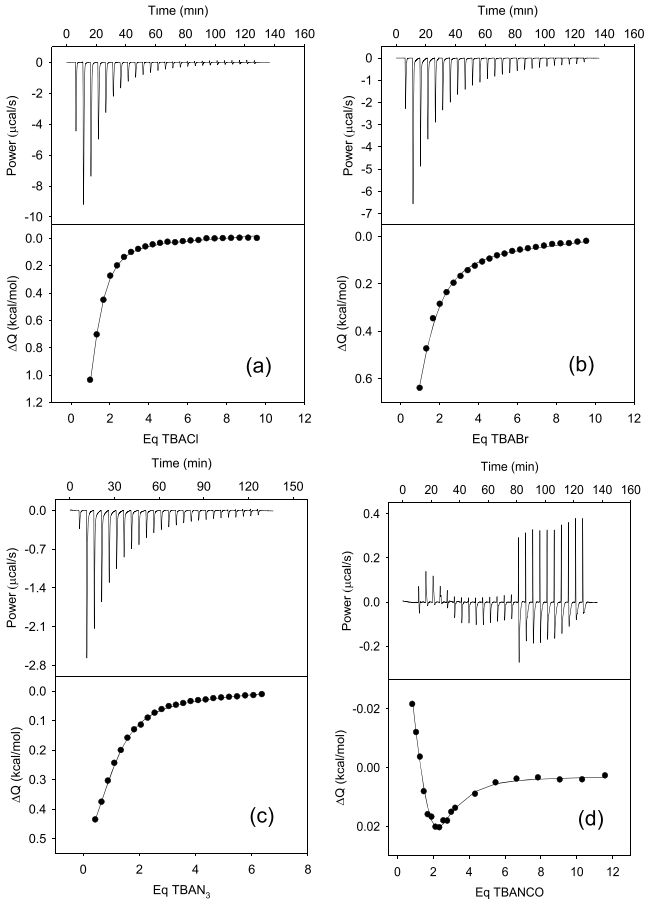

Figure 3. Thermograms and corresponding ITC profiles taken over the course of the titration experiments in DMSO: (a) $[Cu(\mathbf{1})](ClO_4)_2$ (1.0×10^{-3} M) titrated with (TBA)Cl (3.0×10^{-2} M); (b) $[Cu(\mathbf{1})](ClO_4)_2$ (5.1×10^{-3} M) titrated with (TBA)Br (1.4×10^{-1} M); (c) $[Cu(\mathbf{1})](ClO_4)_2$ (5.8×10^{-3} M) titrated with (TBA)N_3 (1.1×10^{-1} M); (d) $[Cu(\mathbf{1})](ClO_4)_2$ (5.8×10^{-3} M) titrated with (TBA)NCO (1.1×10^{-1} M). Circles: experimental data; line: fitting profile (sequential two-site models for (a,b, and d); one-site model for (c); "receptor" complex in the cell); T = 25 °C.

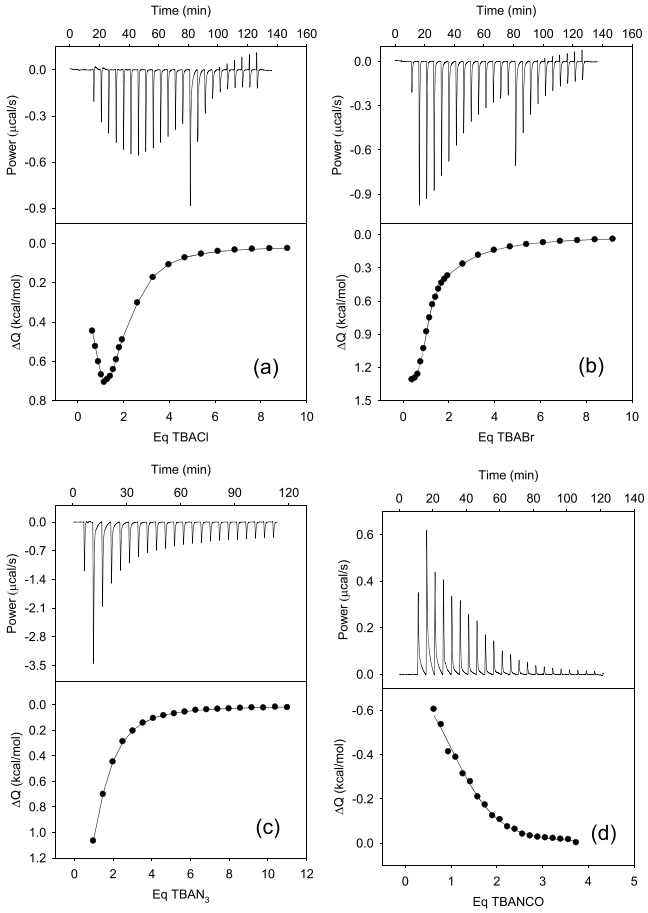

Figure 4. Thermograms and ITC profiles taken over the course of the titration of a solution of $[Cu_2(\mathbf{2})](ClO_4)_4$ (1.0×10^{-3} M) in DMSO with a solution of (a) (TBA)Cl (3.0×10^{-2} M); (b) (TBA)Br (3.0×10^{-2} M); (c) (TBA)N_3 (5.0×10^{-2} M); and (d) (TBA)NCO (3.7×10^{-2} M). Circles: experimental data; line: fitting profile (sequential two-site models for (a, b, and d); one-site model for (c); "receptor" complex in the cell); T = 25 °C.

$$[Cu(1)X]^+ + X^- \rightleftharpoons [Cu(1)X_2] \quad (2)$$

$$(X^- = Cl^-,\ Br^-,\ NCO^-,\ CH_3COO^-)$$

Concerning I^- and N_3^-, the best fitting of the titration data was obtained by assuming the occurrence of only one equilibrium, corresponding to the formation of 1:1 complex species. Although the binding of two anions even for I^- and N_3^- cannot be ruled out, no experimental evidence was obtained for the formation of 1:2 adducts with these anions, i.e., the corresponding stability constant values could be too small to be experimentally determined.

Thermograms and ITC profiles corresponding to the titrations of $[Cu_2(\mathbf{2})]^{4+}$ with Cl^-, Br^-, N_3^-, and NCO^- are reported in Figure 4, whereas data concerning titration with I^- and CH_3COO^- are reported in Figure S5. It should be noted that some of the presented ITC titrations were run with nonconstant additions of a titrant in order to cover a large range of titrant equivalents, while at the same time achieving sufficient resolution in the low [anion]/[complex] region at the beginning of the experiments. Changes in the volume of titrant additions result in visible "spikes" in the corresponding power plots.

Considering the titration with (TBA)N_3, the best fitting of the data can be obtained by assuming the occurrence of one equilibrium corresponding to the formation of a 1:1 complex. On the other hand, when the bimacrocyclic complex is titrated with Cl^-, Br^-, I^-, NCO^-, and CH_3COO^-, the occurrence of two stepwise equilibria (eqs 3 and 4) has to be assumed in order to obtain adequate fitting of the titration data.

$$[Cu_2(2)]^{4+} + X^- \rightleftharpoons [Cu_2(2)X]^{3+} \quad (3)$$

$$[Cu_2(2)X]^{3+} + X^- \rightleftharpoons [Cu_2(2)X_2]^{2+} \quad (4)$$

$$(X^- = Cl^-,\ Br^-,\ I^-,\ NCO^-,\ CH_3COO^-)$$

Differently from the behavior of the di-nickel complex $[Ni_2(\mathbf{2})]^{4+}$ that coordinates up to 3 equiv of anion,[12] the analogous di-copper complex interacts in solution with no more than 2 equiv of anionic ligands.

On the basis of EPR and ITC measurements, the geometrical aspects of the equilibria taking place during the titrations of $[Cu_2(\mathbf{2})]^{4+}$ with the investigated anions in DMSO solution can be hypothesized. They are schematically summarized in Figure 5. The dicopper(II) complex can coordinate anionic species according to two distinct pathways:

DOI: 10.1021/acsomega.8b01710
ACS Omega 2018, 3, 15692−15701

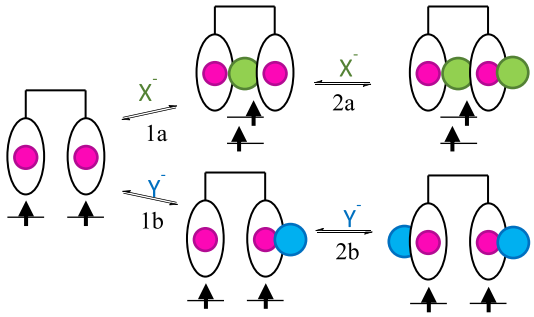

Figure 5. Schematic representation of the equilibria involved over the course of the titration of $[Cu_2(\mathbf{2})](ClO_4)_4$ with (i) bridging anions (X^-, green spheres = Cl^-, Br^-, I^-, and N_3^-), which permit the spin−spin coupling between the two copper centers and (ii) nonbridging anions (Y^-, blue spheres = NCO^-, and CH_3COO^-).

(a) the first anion occupies the inner position between the two macrocyclic subunits, binding two metal centers at the same time (equilibrium 1a in Figure 5), giving rise to a square-pyramidal arrangement for both copper(II) ions and providing a spin−spin coupling as shown by EPR measurements; then, a second equivalent of anion can be coordinated at one of the two equivalent "external" positions of the dinuclear complex (equilibrium 1b in Figure 5), inducing one copper(II) ion to assume an elongated octahedral geometry and preserving the spin−spin coupling;

(b) both the first and the second equivalent of anion interact with $[Cu_2(\mathbf{2})]^{4+}$ at the "external" positions (equilibria 2a and 2b in Figure 5); each metal ion assumes a square-pyramidal positions without inducing any spin−spin coupling.

Taking into account the experimental data and referring to the equilibria depicted in Figure 5, azide interacts with $[Cu_2(\mathbf{2})]^{4+}$ according to equilibrium 1a, chloride, bromide, and iodide according to equilibria 1a and 2a, and cyanate and acetate according to equilibria 1b and 2b.

The thermodynamic quantities (log K, ΔH, and $T\Delta S$) at 25 °C determined by fitting the data obtained during titrations of $[Cu(\mathbf{1})]^{2+}$ and $[Cu_2(\mathbf{2})]^{4+}$ with the considered anions are collected in Table 2. Log K_1 values observed for the interaction of the mononuclear complex with the investigated anions (eq 1) and related to the stability of $[Cu(\mathbf{1})X]^+$ species roughly fall in the 2.0−3.5 range. The experimental affinity sequence is the following:

$$Cl^- > CH_3COO^- > NCO^- > Br^- > N_3^- > I^- \gg SCN^-,\ NO_3^-$$

When the same anionic species are considered, higher equilibrium constants (log K_1 for eq 3) are generally observed for the dinuclear complex than for the mononuclear analogue. This could be expected on the basis of the larger positive charge of $[Cu_2(\mathbf{2})]^{4+}$ than $[Cu(\mathbf{1})]^{2+}$ and also by taking into account the statistical effect in favor of the dicopper(II) complex. Nevertheless, the stability increase of $[Cu_2(\mathbf{2})X]^{3+}$ when compared to $[Cu(\mathbf{1})X]^+$ depends on the anion, it being larger in the case of halides (about 2 order of magnitude) than for azide, acetate, and cyanate (about 0.6−0.7 order of magnitude, see Table 2 and Figure S6). As a consequence, the affinity sequence of the dinuclear complex significantly differs from that observed for the mononuclear analogue:

$$Cl^- > Br^- > I^- \sim CH_3COO \sim NCO^- > N_3^- \gg SCN^-,\ NO_3^-$$

In particular, all halides take the leading positions in the affinity sequence of $[Cu_2(\mathbf{2})]^{4+}$, with bromide overtaking acetate and with cyanate and iodide overtaking azide too. These relevant changes in the affinity of copper(II) bimacrocyclic complex toward anions can be related to the ability of halides to interact with the dinuclear species according to a bridging coordination mode, differently from acetate and cyanate. Therefore, the extra stability displayed by the adducts formed by $[Cu_2(\mathbf{2})]^{4+}$ in the presence of Cl^-, Br^-, or I^- can be explained on the basis of an advantage for the anion in occupying the space between the two metal centers, thus confirming the existence of the bimacrocyclic effect. Quite surprisingly, azide, which according to EPR data also interacts with $[Cu_2(\mathbf{2})]^{4+}$ by bridging the two copper(II) macrocyclic subunits, seems not to benefit from the bimacrocyclic effect as much as halides do. In fact, the stability increase of $[Cu_2(\mathbf{2})N_3]^{3+}$ when compared to $[Cu(\mathbf{1})N_3]^+$ (Δ log K_1 = 0.68) is quite comparable to that observed for the analogue adducts of acetate and cyanate (Δ log K_1 = 0.61 and 0.72, respectively), which are bound only at the "external" coordination positions. It should be noted that, when anions

Table 2. Thermodynamic Parameters at 25 °C Obtained by Fitting ITC Titration Data of $[Cu(\mathbf{1})](ClO_4)_2$ and $[Cu_2(\mathbf{2})](ClO_4)_4$ in DMSO[a]

anion	complex	fitting model	log K_1	ΔH_1 [Kcal mol^{-1}]	$T\Delta S_1$ [Kcal mol^{-1}]	log K_2	ΔH_2 [Kcal mol^{-1}]	$T\Delta S_2$ [Kcal mol^{-1}]
Cl^-	$[Cu(\mathbf{1})]^{2+}$	1:2	3.42(4)	0.97(2)	5.64	1.8(1)	1.14(9)	3.58
	$[Cu_2(\mathbf{2})]^{4+}$	1:2	5.408(6)	0.360(9)	7.73	3.327(6)	1.11(2)	5.65
Br^-	$[Cu(\mathbf{1})]^{2+}$	1:2	2.76(6)	1.31(4)	5.07	1.2(1)	3.06(9)	4.66
	$[Cu_2(\mathbf{2})]^{4+}$	1:2	4.60(1)	1.27(1)	7.54	2.76(1)	1.21(3)	4.97
I^-	$[Cu(\mathbf{1})]^{2+}$	1:1	2.02(3)	2.5(2)	5.20			
	$[Cu_2(\mathbf{2})]^{4+}$	1:2	3.8(2)	1.6(5)	6.73	[b]	[b]	[b]
N_3^-	$[Cu(\mathbf{1})]^{2+}$	1:1	2.54(2)	0.80(2)	4.27			
	$[Cu_2(\mathbf{2})]^{4+}$	1:1	3.220(2)	2.543(4)	6.93			
NCO^-	$[Cu(\mathbf{1})]^{2+}$	1:2	3.1(1)	−0.12(2)	4.18	2.9(2)	0.10(2)	4.10
	$[Cu_2(\mathbf{2})]^{4+}$	1:2	3.82(7)	−1.05(5)	4.16	3.4(4)	0.19(7)	4.77
CH_3COO^-	$[Cu(\mathbf{1})]^{2+}$	1:2	3.25(1)	−0.092(4)	4.33	2.18(2)	−1.51(1)	1.47
	$[Cu_2(\mathbf{2})]^{4+}$	1:2	3.9(1)	−1.6(9)	3.72	3.3(8)	[b]	[b]

[a]In parentheses standard deviations on the last digit. [b]Reliable value cannot be calculated.

DOI: 10.1021/acsomega.8b01710
ACS Omega 2018, 3, 15692−15701

are bound between the two macrocyclic subunits, a rearrangement of the receptor is needed in order to achieve the anion chelation, as also shown by the crystallographic data (see below). These rearrangements may be energetically more costly for azide than for halides; in fact, more substantial conformational changes may be necessary to generate a binding cavity between the two cyclam rings that will not only fit the triatomic azide but also accommodate the geometry imposed by the hybridization of the terminal N donor atoms. As a consequence, the overall stability of $[Cu_2(\mathbf{2})N_3]^{3+}$ and the associated bimacrocyclic effect are significantly reduced.

When the interaction of $[Cu_2(\mathbf{2})X]^{3+}$ with a second equivalent of anion (eq 4) is considered, interestingly, stability constants (i.e., log K_2 values) are very close to those measured for the formation of the corresponding adducts formed by $[Cu(\mathbf{1})]^{2+}$ (i.e., log K_1 for $[Cu(\mathbf{1})X]^{+}$ see Table2 and Figure S7). This is in agreement with the hypothesis that a second anion interacts with the dicopper(II) complex in the same way that the first equivalent of anion interacts with the model mononuclear system.

All interactions between the investigated anions and both copper(II) complexes are characterized by favorable entropy contributions (see Table 2). This result is consistent with the consideration that the reagents are more solvated than the products because the overall charge of the adducts decreases upon anion coordination (see eqs 1 and 3) and, in addition, the complex/anion interaction decreases the surface available for the solvent interaction. In the case of anions that are coordinated according to a bridged mode (Cl^-, Br^-, I^-, and N_3^-) by $[Cu_2(\mathbf{2})]^{4+}$, $T\Delta S_1$ values are distinctly larger than the corresponding $T\Delta S$ term obtained for the mononuclear complex. On the contrary, equilibria involving acetate and cyanate are characterized by $T\Delta S_1$ values that are very similar between mono- and dinuclear complexes (see Table 2 and Figure S8). This indicates that coordination of anionic guest in the space between the two macrocyclic subunits induces a more pronounced anion desolvation with a consequent larger entropy contribution, in agreement with what was previously observed in water.[13]

All enthalpy contributions concerning interactions of both complexes with chloride, bromide, iodide, and azide have positive values. It suggests that exothermic contributions related to the formation of $Cu^{II}-X-Cu^{II}$ coordinative interactions are exceeded by the contrasting endothermic contributions mainly because of (i) desolvation of the anionic guests and the receptor and (ii) rearrangement of the bimacrocyclic receptor toward a face-to-face structure taking place in order to interact with "bridging" anions. On the contrary, negative enthalpy changes were observed in the cases of cyanate and acetate (see Table 2 and Figure S9), which are always coordinated at the "external" positions and do not require a structural modification of the bimacrocyclic complex. However, it can be assumed that the overall endothermic character observed in the interaction of $[Cu_2(\mathbf{2})]^{4+}$ with bridging anions is mainly due to a relevant contribution of the receptor conformational rearrangement.

The examination of enthalpy and entropy terms reported above suggests that the extra stability that characterizes adducts formed by $[Cu_2(\mathbf{2})]^{4+}$ with "bridging anions" (i.e., the bimacrocyclic effect) has a mainly entropic nature. It also can be confirmed that solvation/desolvation processes play an important role in the thermodynamics of anion−bimacrocyclic complex interaction, although differently from what was previously observed in water;[13] in DMSO, these contributions do not completely overshadow the effect because of structural nature of the receptor. In fact, the general "compensatory effect" (i.e., the $T\Delta S/\Delta H$ linear dependence) resulting from a prevalent contribution of solvation/desolvation has not been observed in DMSO.

Spectrophotometric Studies. The affinity toward anions of both mono- and dicopper(II) complexes was also investigated through spectrophotometric titration experiments. Solutions of $[Cu(\mathbf{1})](ClO_4)_2$ and $[Cu_2(\mathbf{2})](ClO_4)_4$ in DMSO were titrated with standard solutions of the TBA^+ salts of the investigated anions (Cl^-, Br^-, I^-, N_3^-, NCO^-, CH_3COO^-, SCN^-, and NO_3^-). The titration data were fitted by means of a nonlinear least-squares program (HypSpec),[16] in order to identify the species present at the equilibrium and to obtain the association constants (see Table S1 and Figures S10−S12).

Although some stability constants cannot be determined by spectrophotometric titrations because of unreliable data fittings, the results obtained by UV−vis titrations are generally in good agreement with those found by ITC experiments (see Tables 2 and S1). In particular, when the interaction with "bridging" anions is considered, the differences between log K_1 values determined for $[Cu_2(\mathbf{2})]^{4+}$ and $[Cu(\mathbf{1})]^{2+}$ are similar to those obtained by ITC experiments. It confirms that the dicopper(II) complex, thanks to its "chelating" ability, provides an extra stability (i.e., the bimacrocyclic effect) to the adducts with anionic guests that fit the space between the two macrocyclic subunits and coordinate the two copper(II) ions according to the bridging mode.

X-ray Crystallography. The molecular structure of the $[Cu_2(\mathbf{2})N_3]^{3+}$ molecular cation present in the $[Cu_2(\mathbf{2})N_3(ClO_4)_2](ClO_4)\cdot 0.5(H_2O)$ crystalline complex salt is shown in Figure 6. For comparison, the structure of $[Cu_2(\mathbf{2})Br]^{3+}$ is also reported.[13] A plot showing thermal ellipsoids is drawn in Figure S13 (see Supporting Information).

As expected, the two facing cyclam moieties are arranged in a trans-III (RRSS) configuration. The observed mean distances between copper ions and secondary amine nitrogen atoms [$Cu^{II}-N_{amine}$: 2.02(1) and 2.03(1) Å] are similar to that observed in the corresponding bromide adduct[13] and correspond to that expected for a strain-free Cu−N bond in cyclam and cyclam-like macrocycles.[17] The two metal centers are displaced by 0.13(1) and 0.15(1) Å from the equatorial N_4 best plane and point toward the inside of the receptor cavity that contains the azide ion. The two observed $Cu^{II}-N_{azide}$ distances are 2.31(1) and 2.30(1) Å, whereas the $Cu^{II}\cdots Cu^{II}$ separation is 6.14(1) Å. The axially elongated octahedral coordination arrangements for both metal centers are completed by two O atoms of two perchlorate groups, placed at rather long distances of 2.73(1) and 2.75(1) Å.

Differently from what we observed in the structure of the analogous bromide adduct,[13] in $[Cu_2(\mathbf{2})N_3]^{3+}$ the coordination of azide in the inner position between the two metal ions occurs through a significant rearrangement of the bimacrocycle conformation. In fact, it loses the C_s molecular symmetry observed in the bromide adduct and originates a complex species lacking any molecular symmetry. In this way, the chelation of azide by the dicopper(II) complex originates two $Cu^{II}-N-N$ bond angles of 114(1)° and 137(1)° with respect to the two terminal azide atoms (see Figure 6). Such an arrangement favors the bonding requirements of two nitrogen atoms having a prevailing sp^2 nature. As a result, the nearly linear azide ligand is almost coplanar with the best plane of the

DOI: 10.1021/acsomega.8b01710
ACS Omega 2018, 3, 15692−15701

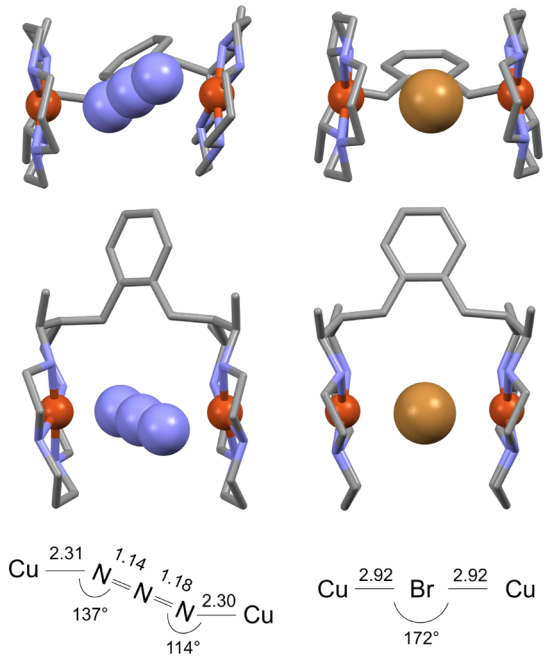

Figure 6. Simplified sketches of the $[Cu_2(\mathbf{2})]^{4+}$ bimacrocyclic complex interacting with azide (left) and bromide (right) ions placed in the inner positions. Bond distances (Å) and angles for the metal–anion interactions are reported at the bottom. Additional perchlorate counterions (for the azide complex) and bromide ions (for the bromide complex) completing the elongated octahedral coordination for the Cu^{II} centers are not shown.

aromatic spacer and the angle between the azide molecular axis and the C_6 aromatic best plane is about 5°.

The structural differences from the analogous bromide adduct are clearly evident when some specific features are considered: $[Cu_2(\mathbf{2})Br]^{3+}$ displays a shorter $Cu^{II}\cdots Cu^{II}$ separation [5.83(1) Å] and the inner bromide promotes an almost linear bridging coordination arrangement with a Cu^{II}–Br–Cu^{II} angle of 171.7(1)° (Figure 6).

In the solid state, copper(II) centers of adjacent bimacrocyclic units are not directly bridged by the perchlorate counterion. Instead, the crystal is supported by weak NH···O and unconventional CH···O interactions in which O atoms from the perchlorate anions act as H-acceptors (Figure S14).

CONCLUSIONS

The dicopper(II) complex investigated in this work, $[Cu_2(\mathbf{2})]^{4+}$, containing two subunits of cyclam-like copper(II) complex and an *o*-xylyl spacer, interacts with selected anions (i) according to a bridging coordination mode with the substrate that binds the two metal centers at the same time between the two macrocyclic subunits that face each other or (ii) by interacting with anions only at the "external" coordination positions of copper(II) ions. The bridging coordination mode is demonstrated by X-ray crystallographic data and by EPR experiments. In fact, bridged anions (Cl^-, Br^-, I^-, and N_3^-) force the two metal centers within close proximity and induce spin–spin coupling. Determination of stability constants and related thermodynamic parameters by UV–vis and ITC titration experiments shows that, when anions are bound according to the bridging mode, the corresponding 1:1 adducts are considerably more stable than the corresponding 1:1 adducts formed by the monomacrocyclic reference complex $[Cu(\mathbf{1})]^{2+}$. This paper confirms that the "chelation" of an anionic substrate by a bimacrocyclic complex provides an extra stability to the resulting adduct, which can be described as a "bimacrocyclic effect", as previously proposed for the analogous dinickel(II) complex. The observed extra stability has mainly an entropic nature in the case of interaction with halides. The adduct with azide also benefits from a favorable entropic effect, but it is significantly mitigated by an enthalpic disadvantage, which could be due to a more difficult host rearrangement when compared to the analogous bridged halide species. The examination of entropy and enthalpy terms points out that the contribution ascribed to solvation/desolvation, which is prevalent in water, does not completely overshadow the contribution of receptor structural features when the anion–receptor interaction is studied in polar nonaqueous media. In fact, the general "compensatory effect" observed when the interaction of $[Cu_2(\mathbf{2})]^{4+}$ with anions was studied in water cannot be observed in DMSO.

EXPERIMENTAL SECTION

General Procedures and Materials. Unless otherwise stated, all reagents and solvents were supplied by Sigma-Aldrich and used as received. All TBA^+ salts were of greater than 98% purity and dried in vacuo overnight before use. DMSO (ACS reagent, ≥99.9%) was purchased in small septum cap bottles (water content <0.005%) and was properly handled to avoid as much as possible the absorption of humidity from air. Mass spectra were acquired on a Thermo-Finnigan ion-trap LCQ Advantage Max instrument equipped with an ESI source. IR spectra were run on a PerkinElmer Spectrum X100 Fourier transform infrared (FT-IR) instrument equipped with an attenuated total reflectance (U-ATR) apparatus. UV–vis spectra were recorded using a Varian Cary 50 or Cary 100 spectrophotometer with a quartz cuvette (path length: 1 or 0.1 cm).

Synthesis of Copper(II) Complexes. $[Cu(\mathbf{1})](ClO_4)_2$ and $[Cu_2(\mathbf{2})](ClO_4)_4$ were prepared according to a three-step procedure: (i) synthesis of $[Ni(\mathbf{1})](ClO_4)_2$[18] and $[Ni_2(\mathbf{2})](ClO_4)_4$[10,19] according to previously reported procedures; (ii) demetalation of nickel(II) complexes and isolation of free ligands **1**[18] and **2**;[10] and (iii) reaction of free ligands **1** and **2** with $Cu(ClO_4)_2\cdot 6H_2O$ providing mono- and dinuclear copper(II) complexes.

*[(5,7-Dimethyl-6-benzyl-1,4,8,11-tetraazacyclotetradecane)-copper(II)]perchlorate, [Cu(**1**)](ClO$_4$)$_2$.* Free ligand **1** (0.06 g, 0,19 mmol) was dissolved in a mixture of MeOH (10 mL) and aqueous 3 M $HClO_4$ (1 mL), then excess $Cu(ClO_4)_2\cdot 6H_2O$ (0.8 g, 2.2 mmol) was added. The resulting solution was refluxed for 2 h and a purple precipitate was formed. After cooling to room temperature, the purple powder was collected by filtration and recrystallized from MeOH. Yield: 0.11 g (~100%). MS (CH_3OH, ESI): *m*/*z* 190.69 (100%, $[Cu^{II}(\mathbf{1})]^{2+}$), 380.35 (20%, $[Cu^{II}(\mathbf{1})-H^+]^+$). UV–vis [DMSO, λ_{max} nm (ε, M^{-1} cm^{-1})]: 535 (98). FT-IR (cm^{-1}): 3235, 2975, 2935, 2885, 1460, 1420, 1070, 980, 750, 620.

*α,α′-Bis[(5,7-dimethyl-1,4,8,11-tetraazacyclotetradecan-6-yl)-copper(II)]-o-xylene perchlorate, [Cu$_2$(**2**)](ClO$_4$)$_4$.* Free ligand **2** (0.1 g, 0,18 mmol) was dissolved in a mixture of MeOH (20 mL) and aqueous 3 M $HClO_4$ (1 mL), then $Cu(ClO_4)_2\cdot 6H_2O$ (1.5 g, 0.4 mmol) was added. The resulting solution was refluxed for 2 h and, after cooling to room temperature, a purple-colored precipitate was collected by filtration and recrystallized from MeOH. Yield: 0.19 g

DOI: 10.1021/acsomega.8b01710
ACS Omega 2018, 3, 15692–15701

(~100%). MS (CH_3OH, ESI): m/z 391.19 (100%, $[Cu_2^{II}(\mathbf{2})-H^+ + ClO_4^-]^{2+}$. UV−vis [DMSO, λ_{max} nm (ε, M^{-1} cm^{-1})]: 535 (231). FT-IR (cm^{-1}): 3235, 2975, 2885, 1470, 1440, 1080, 1000, 980, 745, 620.

EPR Studies. The EPR spectra were recorded at 120 K and 31.81 mW microwave power with a field modulation amplitude of 5 G. The spectrometer was Bruker EMX-10/12 (Bruker BioSpin GmbH, Karlsruhe, Germany) operating in the X-band and equipped with a ER4119HS cavity and temperature control. The spectral simulations were made using the Bruker WinEPR Simfonia package.

Isothermal Titration Calorimetry. ITC titrations were performed by using a nano ITC low-volume isothermal titration calorimeter (TA instrument). All titrations were performed at 25 °C in DMSO by adding the anionic titrants (DMSO solutions of TBA^+ salts) to the solution of the envisaged complex, placed in the instrument sample cell. The association parameters (K, ΔH, and ΔS), as well as the interaction stoichiometry, were determined by a fitting procedure using AFFINImeter software.[15] Blank titrations in DMSO were performed and subtracted from the corresponding titrations with anions to remove the effect of titrant dilution.

UV−Vis Spectrophotometry. UV−vis spectra were recorded on a Varian CARY 50 spectrophotometer with a quartz cuvette of 1 cm path length. UV−vis titrations were performed at 25 °C on DMSO solutions of $[Cu(\mathbf{1})](ClO_4)_2$ and $[Cu_2(\mathbf{2})](ClO_4)_4$ (1×10^{-3} M), by adding aliquots of freshly prepared standard solutions (in DMSO) of (TBA)X (X = Cl, Br, I, NCO, NCS, N_3, NO_3, and CH_3COO). Titration data were processed with HypSpec software (Hyperquad suite) to determine the equilibrium constants.[16] Best fitting of titration data was evaluated on the basis of the χ^2 value: accepted models showed χ^2 values lower than 10 and rejected models showed $\chi^2 > 50$. The HySS program was used to obtain the distribution diagrams of the species.[20]

X-ray Crystallographic Study. Crystals of the complex salt $[Cu_2(\mathbf{2})N_3(ClO_4)_2](ClO_4)\cdot 0.5(H_2O)$, suitable for crystallographic studies, were obtained by slow diffusion of EtOH vapors in a 50:50 MeCN/H_2O solution of $[Cu_2(\mathbf{2})](ClO_4)_4$ in the presence of excess NaN_3. Diffraction data for the $[Cu_2(\mathbf{2})N_3(ClO_4)_2](ClO_4)\cdot 0.5(H_2O)$ (violet, prismatic, 0.30 × 0.16 × 0.10 mm^3) crystal were collected by means of a Bruker AXS CCD-based three-circle diffractometer, working at ambient temperature with graphite-monochromatized Mo Kα X-radiation (λ = 0.7107 Å). Data reductions were performed with SAINT software[21] and intensities were corrected for Lorentz and polarization effects. Absorption effects were empirically evaluated by SADABS software[22] and absorption corrections were applied to the data. Crystal structures were solved by direct methods (SIR 97)[23] and refined by full-matrix least-squares procedures on F^2 using all reflections (SHELXL 2018/1).[24] All hydrogen atoms were placed at calculated positions with the appropriate AFIX instructions and were refined using a riding model. Anisotropic displacement parameters were refined for all nonhydrogen atoms. Perchlorate counterions that are not bonded to metal centers exhibited positional disorder, resolved by placing the Cl species and one O specie in two-half populated atom sites and using soft geometrical restraint on perchlorate's bond distances and bond angles. Soft geometrical restraints were also used for the other perchlorate counterions, probably affected by an unresolved positional disorder. CCDC 1847728 contains the supplementary crystallographic data for this paper. These data can be obtained free of charge from the Cambridge Crystallographic Data Centre.

Crystal data for $[Cu_2(\mathbf{2})N_3(ClO_4)_2](ClO_4)\cdot 0.5(H_2O)$. $C_{32}H_{63}Cl_3Cu_2N_{11}O_{12.5}$, M = 1035.36, orthorhombic, Pbcn (no. 60), a = 24.6695(14) Å, b = 18.6531(10) Å, c = 20.3858(11) Å, V = 9380.8(9) $Å^3$, Z = 8, 85 937 measured reflections, 8271 unique reflections (R_{int} 0.041), 6100 strong data [$I_O > 2\sigma(I_O)$], 0.0777 and 0.2285 R_1 and wR_2 for strong data, 0.0966 and 0.2609 R_1 and wR_2 for all data.

■ ASSOCIATED CONTENT

Supporting Information

The Supporting Information is available free of charge on the ACS Publications website at DOI: 10.1021/acsomega.8b01710.

Additional figures concerning EPR spectra, thermograms and profiles from ITC titration experiments, bar diagrams comparing thermodynamic parameters for different anion−complex interactions, absorption spectra and corresponding profiles from UV−vis titration experiments, plot showing thermal ellipsoids of the $[Cu_2(\mathbf{2})N_3(ClO_4)_2](ClO_4)\cdot 0.5(H_2O)$ molecular structure, and simplified sketch showing intra- and intermolecular connections in the solid state structure of the azide adduct (PDF)

Crystallographic data of the copper(II) bicyclam complex (CIF)

■ AUTHOR INFORMATION

Corresponding Authors

*E-mail: luigi.fabbrizzi@unipv.it (L.F.).
*E-mail: maurizio.licchelli@unipv.it (M.L.).
*E-mail: marco.bonizzoni@ua.edu (M.B.).

ORCID

Maurizio Licchelli: 0000-0002-9276-1530
Marco Bonizzoni: 0000-0003-0155-5481

Notes

The authors declare no competing financial interest.

■ ACKNOWLEDGMENTS

M.B. acknowledges support from the U.S. National Science Foundation (grant OIA-1632825).

■ REFERENCES

(1) (a) Park, C. H.; Simmons, H. E. Macrobicyclic amines. III. Encapsulation of halide ions by in,in-1,(k + 2)-diazabicyclo[k.l.m.]-alkane ammonium ions. *J. Am. Chem. Soc.* **1968**, *90*, 2431−2432. (b) Lehn, J. M.; Sonveaux, E.; Willard, A. K. Molecular recognition. Anion cryptates of a macrobicyclic receptor molecule for linear triatomic species. *J. Am. Chem. Soc.* **1978**, *100*, 4914−4916. (c) *Anion Coordination Chemistry*; Bowman-James, K.; Bianchi, A.; García-España, E., Eds.; John Wiley & Sons: New York, 2012. (d) Gale, P. A.; Howe, E. N. W.; Wu, X. Anion Receptor Chemistry. *Chem* **2016**, *1*, 351−422.

(2) (a) Schmidtchen, F. P.; Berger, M. Artificial Organic Host Molecules for Anions. *Chem. Rev.* **1997**, *97*, 1609−1646. (b) Snowden, T. S.; Anslyn, E. V. Anion recognition: synthetic receptors for anions and their application in sensors. *Curr. Opin. Chem. Biol.* **1999**, *3*, 740−746. (c) Bondy, C. R.; Loeb, S. J. Amide based receptors for anions. *Coord. Chem. Rev.* **2003**, *240*, 77−99. (d) Choi, K.; Hamilton, A. D. Macrocyclic anion receptors based on directed hydrogen bonding interactions. *Coord. Chem. Rev.* **2003**, *240*, 101−110. (e) Langton, M.

DOI: 10.1021/acsomega.8b01710
ACS Omega 2018, 3, 15692−15701

J.; Robinson, S. W.; Marques, I.; Félix, V.; Beer, P. D. Halogen bonding in water results in enhanced anion recognition in acyclic and rotaxane hosts. *Nat. Chem.* **2014**, *6*, 1039−1043. (f) Gale, P. A.; Caltagirone, C. Anion sensing by small molecules and molecular ensembles. *Chem. Soc. Rev.* **2015**, *44*, 4212−4227. (g) Kubik, S. Anion recognition in aqueous media by cyclopeptides and other synthetic receptors. *Acc. Chem. Res.* **2017**, *50*, 2870−2878.

(3) (a) Comarmond, J.; Plumere, P.; Lehn, J. M.; Agnus, Y.; Louis, R.; Weiss, R.; Kahn, O.; Morgenstern-Badarau, I. Dinuclear copper(II) cryptates of macrocyclic ligands: synthesis, crystal structure, and magnetic properties. Mechanism of the exchange interaction through bridging azido ligands. *J. Am. Chem. Soc.* **1982**, *104*, 6330−6340. (b) Drew, M. G. B.; Hunter, J.; Marrs, D. J.; Nelson, J.; Harding, C. Cascade complexes of an octaaza cryptand: co-ordinated azide with linear M-NNN-M geometry. *J. Chem. Soc., Dalton Trans.* **1992**, 3235−3242. (c) O'Neil, E. J.; Smith, B. D. Anion recognition using dimetallic coordination complexes. *Coord. Chem. Rev.* **2006**, *250*, 3068−3080. (d) Ngo, H. T.; Liu, X.; Jolliffe, K. A. Anion recognition and sensing with Zn(ii)-dipicolylamine complexes. *Chem. Soc. Rev.* **2012**, *41*, 4928−4965. (e) Butler, S. J.; Parker, D. Anion binding in water at lanthanide centres: from structure and selectivity to signalling and sensing. *Chem. Soc. Rev.* **2013**, *42*, 1652−1666. (f) Carreira-Barral, I.; Rodríguez-Blas, T.; Platas-Iglesias, C.; de Blas, A.; Esteban-Gómez, D. Cooperative Anion Recognition in Copper(II) and Zinc(II) Complexes with a Ditopic Tripodal Ligand Containing a Urea Group. *Inorg. Chem.* **2014**, *53*, 2554−2568. (g) Aletti, A. B.; Gillen, D. M.; Gunnlaugsson, T. Luminescent/colorimetric probes and (chemo-) sensors for detecting anions based on transition and lanthanide ion receptor/binding complexes. *Coord. Chem. Rev.* **2018**, *354*, 98−120.

(4) Boiocchi, M.; Licchelli, M.; Milani, M.; Poggi, A.; Sacchi, D. Oxo-Anion Recognition by Mono- and Bisurea Pendant-Arm Macrocyclic Complexes. *Inorg. Chem.* **2015**, *54*, 47−58.

(5) (a) Fabbrizzi, L.; Poggi, A. Anion recognition by coordinative interactions: metal-amine complexes as receptors. *Chem. Soc. Rev.* **2013**, *42*, 1681−1699. (b) Amendola, V.; Fabbrizzi, L.; Licchelli, M.; Taglietti, A. Anion sensing by fluorescence quenching or revival. In *Anion Coordination Chemistry*; Bowman-James, K.; Bianchi, A.; Garcia-Espana, E., Eds.; John Wiley & Sons: New York, 2012, pp 521-552. (c) Bonizzoni, M. Fluorescent sensors based on indicator displacement. In *Comprehensive Supramolecular Chemistry II*; Atwood, J. L., Ed.; Elsevier: Amsterdam, 2017; pp 21−36.

(6) (a) Fabbrizzi, L.. A Lifetime Walk in the Realm of Cyclam. In *Macrocyclic and Supramolecular Chemistry: How Izatt-Christensen Award Winners Shaped the Field*; Izatt, R. M., Ed.; Wiley: New York, 2016; pp 165−199. (b) Cabbiness, D. K.; Margerum, D. W. Effect of macrocyclic structures on the rate of formation and dissociation of copper(II) complexes. *J. Am. Chem. Soc.* **1970**, *92*, 2151−2153.

(7) (a) Lehn, J. M.; Pine, S. H.; Watanabe, E.; Willard, A. K. Binuclear cryptates. Synthesis and binuclear cation inclusion complexes of bis-tren macrobicyclic ligands. *J. Am. Chem. Soc.* **1977**, *99*, 6766−6768. (b) Lachkar, M.; Guilard, R.; Atmani, A.; De Cian, A.; Fischer, J.; Weiss, R. Synthesis of new binucleating cylindrical macrotricyclic ligands where two cyclam rings are in a face-to-face conformation. Characterization of their dicopper(II) and dinickel(II) complexes. *Inorg. Chem.* **1998**, *37*, 1575−1584. (c) Fabbrizzi, L.; Leone, A.; Taglietti, A. A Chemosensing Ensemble for Selective Carbonate Detection in Water Based on Metal-Ligand Interactions. *Angew. Chem. Int. Ed.* **2001**, *40*, 3066−3069; *Angew. Chem.* **2001**, *113*, 3156−3159.

(8) Mochizuki, K.; Manaka, S.; Takeda, I.; Kondo, T. Synthesis and Structure of [6,6'-Bi(5,7-dimethyl-1,4,8,11-tetraazacyclotetradecane)] dinickel(II) Triflate and Its Catalytic Activity for Photochemical CO_2 Reduction. *Inorg. Chem.* **1996**, *35*, 5132−5136.

(9) Fukuzumi, S.; Okamoto, K.; Gros, C. P.; Guilard, R. Mechanism of four-electron reduction of dioxygen to water by ferrocene derivatives in the presence of perchloric acid in benzonitrile, catalyzed by cofacial dicobalt porphyrins. *J. Am. Chem. Soc.* **2004**, *126*, 10441−10449.

(10) Kajiwara, T.; Yamaguchi, T.; Kido, H.; Kawabata, S.; Kuroda, R.; Ito, T. A dinucleating bis(dimethylcyclam) ligand and its dinickel(II) and dizinc(II) complexes with the face-to-face ring arrangement. *Inorg. Chem.* **1993**, *32*, 4990−4991.

(11) Szacilowski, K. T.; Xie, P.; Malkhasian, A. Y. S.; Heeg, M. J.; Udugala-Ganehenege, M. Y.; Wenger, L. E.; Endicott, J. F. Solid-state structures and magnetic properties of halide-bridged, face-to-face bis-nickel(II)-macrocyclic ligand complexes: ligand-mediated interchanges of electronic configuration. *Inorg. Chem.* **2005**, *44*, 6019−6033.

(12) Boiocchi, M.; Fabbrizzi, L.; Fusco, N.; Invernici, M.; Licchelli, M.; Poggi, A. Anion Binding by Dimetallic Nickel(II) and Nickel(III) Complexes of a Face-to-Face Bicyclam: Looking for a Bimacrocyclic Effect. *Inorg. Chem.* **2016**, *55*, 2946−2959.

(13) Boiocchi, M.; Bonizzoni, M.; Ciarrocchi, C.; Fabbrizzi, L.; Invernici, M.; Licchelli, M. Anion Recognition in Water, Including Sulfate, by a Bicyclam Bimetallic Receptor: A Process Governed by the Enthalpy/Entropy Compensatory Relationship. *Chem.—Eur. J.* **2018**, *24*, 5659−5666.

(14) (a) Ghachtouli, S. E.; Cadiou, C.; Déchamps-Olivier, I.; Chuburu, F.; Aplincourt, M.; Turcry, V.; Le Baccon, M.; Handel, H. Spectroscopy and redox behaviour of dicopper(II) and dinickel(II) complexes of bis (cyclen) and bis (cyclam) ligands. *Eur. J. Inorg. Chem.* **2005**, *2005*, 2658−2668. (b) Schweinfurth, D.; Khusniyarov, M. M.; Bubrin, D.; Hohloch, S.; Su, C.-Y.; Sarkar, B. Tuning Spin-Spin Coupling in Quinonoid-Bridged Dicopper(II) Complexes through Rational Bridge Variation. *Inorg. Chem.* **2013**, *52*, 10332−10339. (c) Gaudette, A. I.; Jeon, I.-R.; Anderson, J. S.; Grandjean, F.; Long, G. J.; Harris, T. D. Electron Hopping through Double-Exchange Coupling in a Mixed-Valence Diiminobenzoquinone-Bridged Fe_2 Complex. *J. Am. Chem. Soc.* **2015**, *137*, 12617−12626.

(15) Freiburger, L.; Auclair, K.; Mittermaier, A. Global ITC fitting methods in studies of protein allostery. *Methods* **2015**, *76*, 149−161 . (as implemented in the AFFINImeter ITC software, https://www.affinimeter.com) .

(16) (a) Gans, P.; Sabatini, A.; Vacca, A. Investigation of equilibria in solution. Determination of equilibrium constants with the HYPERQUAD suite of programs. *Talanta* **1996**, *43*, 1739−1753. (b) Gans, P.; Sabatini, A.; Vacca, A. Determinations of equilibrium constants from spectrophotometric data obtained from solutions of known pH: the program pHab. *Ann. Chim.* **1999**, *89*, 45−49 ; http://www.hyperquad.co.uk/HypSpec2014.htm .

(17) Thoem, V. J.; Boeyens, J. C. A.; McDougall, G. J.; Hancock, R. D. Origin of the high ligand field strength and macrocyclic enthalpy in complexes of nitrogen-donor macrocycles. *J. Am. Chem. Soc.* **1984**, *106*, 3198−3207.

(18) DeRosa, F.; Bu, X.; Pohaku, K.; Ford, P. C. Synthesis and Luminescence Properties of Cr(III) Complexes with Cyclam-Type Ligands Having Pendant Chromophores, trans-[Cr(L)Cl_2]Cl. *Inorg. Chem.* **2005**, *44*, 4166−4174.

(19) Kajiwara, T.; Yamaguchi, T.; Oshio, H.; Ito, T. Synthesis, Structure, and Magnetic Property of Linear Chloro-Bridged Nickel-(II) Tetramer with Dinucleating Bis-dimethylcyclam Ligand. *Bull. Chem. Soc. Jpn.* **1994**, *67*, 2130−2135.

(20) Alderighi, L.; Gans, P.; Ienco, A.; Peters, D.; Sabatini, A.; Vacca, A. Hyperquad simulation and speciation (HySS): a utility program for the investigation of equilibria involving soluble and partially soluble species. *Coord. Chem. Rev.* **1999**, *184*, 311−318 ; http://www.hyperquad.co.uk/hyss.htm .

(21) *SAINT Software Reference Manual*, Version 6; Bruker AXS Inc.: Madison, WI, 2003.

(22) Krause, L.; Herbst-Irmer, R.; Sheldrick, G. M.; Stalke, D. Comparison of silver and molybdenum microfocus X-ray sources for single-crystal structure determination. *J. Appl. Crystallogr.* **2015**, *48*, 3−10.

(23) Altomare, A.; Burla, M. C.; Camalli, M.; Cascarano, G. L.; Giacovazzo, C.; Guagliardi, A.; Moliterni, A. G. G.; Polidori, G.;

DOI: 10.1021/acsomega.8b01710
ACS Omega 2018, 3, 15692−15701

Spagna, R. SIR97: a new tool for crystal structure determination and refinement. *J. Appl. Crystallogr.* **1999**, *32*, 115−119.
(24) Sheldrick, G. M. Crystal structure refinement withSHELXL. *Acta Crystallogr., Sect. C: Struct. Chem.* **2015**, *71*, 3−8.

DOI: 10.1021/acsomega.8b01710
ACS Omega 2018, 3, 15692−15701